

The $^{27}\text{Al}(p, \alpha)^{24}\text{Mg}$ and $^{27}\text{Al}(p, \gamma)^{28}\text{Si}$ reactions at astrophysical energies: first time observation of the 84 keV resonance

Marco La Cognata^{1,*}

¹Laboratori Nazionali del Sud, Istituto Nazionale di Fisica Nucleare, 95123 Catania, Italy

Abstract. The ^{26}Al abundance represents a key diagnostic tool, serving as a tracer of ongoing nucleosynthesis throughout the Galaxy and providing constraints on the rate of Galactic core-collapse supernovae. Quantification of this abundance relies on the analysis of the ^{26}Mg excess relative to ^{24}Mg in meteorites and on the detection of the 1809 keV γ -ray line using space-borne telescopes, and is usually normalized to the ^{27}Al abundance. Consequently, precise isotopic measurements of stable aluminum and magnesium are essential. These elements also participate in the Mg-Al cycle, responsible for synthesizing Al and Mg in stellar interiors. Spectroscopic observations of globular-cluster red giants have revealed systematic Mg-Al anticorrelations, providing evidence for multiple stellar populations and necessitating additional observational and theoretical work. Central to understanding these astrophysical phenomena is the characterization of the $^{27}\text{Al}(p, \alpha)^{24}\text{Mg}$ and $^{27}\text{Al}(p, \gamma)^{28}\text{Si}$ nuclear reactions, which constitute the primary destruction channels for ^{27}Al . The extraordinarily small cross sections at astrophysically relevant energies present significant challenges for direct laboratory measurements, resulting in substantial uncertainties. The Trojan Horse Method provides an alternative experimental approach, enabling the investigation of these reactions at energies below 100 keV. This technique has led to the determination of the 84 keV resonance strength and the establishment of improved upper limits for nearby resonances. The resulting reaction rates are lower by factors approaching 3 compared to the values currently implemented in astrophysical models, with significant implications for nucleosynthesis calculations in massive stars.

1 The $^{27}\text{Al}(p, \alpha)^{24}\text{Mg}$ measurement

1.1 The astrophysical motivation

Measurements of magnesium and aluminum isotopic abundances are fundamental to numerous astrophysical investigations. Recent high-resolution spectroscopic studies of globular cluster red-giant-branch stars (e.g., NGC 2808, ω -Cen, M4) have revealed systematic Mg-Al anticorrelations, suggesting multiple stellar populations and requiring refined theoretical frameworks [1, 2]. The production and destruction of ^{24}Mg exhibits strong temperature sensitivity in the narrow range $0.7 \times 10^8 \leq T \leq 0.8 \times 10^8$ K during stellar hydrogen burning [3].

These isotopes participate in the Mg-Al cycle (see Fig.1), characteristic of high-temperature ($T \sim 0.55 \times 10^8$ K) hydrogen burning in evolved stars [4]. Although less significant than the CNO cycle for stellar energy generation due to higher Coulomb barriers, the Mg-Al cycle substantially influences the magnesium and aluminum nucleosynthesis. The $^{27}\text{Al}(p, \alpha)^{24}\text{Mg}$ reaction governs ^{27}Al destruction and ^{24}Mg production. Cycle closure depends on the competition with $^{27}\text{Al}(p, \gamma)^{28}\text{Si}$, where the (p, α) rate dominates above 10^9 K but only marginally exceeds the (p, γ) rate between $0.3 - 0.8 \times 10^8$ K, with substantial uncertainties affecting astrophysical modeling [5].

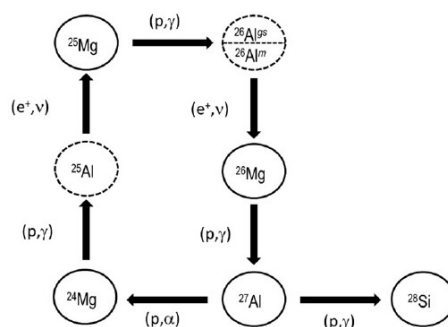


Figure 1. Schematic view of the Mg-Al cycle, including the $^{27}\text{Al}(p, \gamma)^{28}\text{Si}$ channel responsible of the leakage from the Mg-Al cycle toward silicon.

Galactic ^{26}Al abundance, determined through INTEGRAL observations of 1809 keV γ -ray emission [6] and ^{26}Mg excesses in presolar grains and meteorites [7], provides constraints on nucleosynthesis. While massive stars and supernova progenitors represent likely ^{26}Al sources [8], asymptotic giant branch stars contribute significantly to abundances in Al-rich dust [9]. Improved proton-capture reaction measurements at hydrogen-burning energies could substantially refine these nucleosynthesis scenarios as well.

*e-mail: lacognata@lns.infn.it

1.2 State of the art

The currently adopted uncertainty on the $^{27}\text{Al}(p, \alpha)^{24}\text{Mg}$ reaction rate from previous work spans nearly one order of magnitude at $T = 10^8$ K, with values ranging from 1.85×10^{-11} to 8.51×10^{-11} $\text{cm}^3 \text{mol}^{-1} \text{s}^{-1}$, and uncertainties increasing substantially at lower temperatures [10]. This rate evaluation relies on direct experimental measurements, compiled spectroscopic information, transfer-reaction-derived branching ratios, and shell-model predictions [11–14]. The challenge in establishing reliable rates stems from over 90 resonances occurring below $E_{\text{cm}} \leq 3$ MeV.

Direct measurements in the 200–360 keV range provided upper bounds for the resonance strengths [11], while spectroscopic compilations form the basis of rate calculations, though much of this data is outdated with limited coverage of astrophysically relevant energies [12]. Transfer reaction studies using $^{27}\text{Al}(^3\text{He}, d)^{28}\text{Si}$ established additional constraints by populating ^{28}Si states near the proton-emission threshold [13]. Previous analyses [15] already revealed large deviations from earlier recommendations [16], with uncertainties reaching three orders of magnitude below $T \sim 0.3 \times 10^8$ K.

The most relevant advancement in recent evaluations involved implementing Monte Carlo techniques for statistically rigorous uncertainty propagation from individual resonance parameters to total rates [17]. Given the need for updated measurements at astrophysically relevant energies and the potential implications for aluminum nucleosynthesis in low-mass stellar hydrogen burning, new indirect measurements using the Trojan Horse Method were undertaken to refine the STARLIB reaction rate library.

1.3 The method and the experiment

Indirect methodologies enable the determination of astrophysical S-factors by measuring cross sections of related processes and applying nuclear reaction theory to establish connections between them (see, for instance, the $^{13}\text{C}(\alpha, n)^{16}\text{O}$ reaction [18]). The Trojan Horse Method (THM) [19] represents such an experimental indirect approach, successfully employed to investigate numerous astrophysically significant reactions through three-body quasi-free processes.

In this investigation, a ^{27}Al projectile beam impinges on a deuteron target, characterized by its simple $p+n$ structure with predominantly s -wave motion. Under specifically selected kinematic conditions, ^{27}Al interacts exclusively with the participant nucleon while the spectator nucleon remains uninvolved, enforced through small relative momenta corresponding to large internucleon separations. This quasi-free interaction populates ^{28}Si excited states, subsequently decaying into the $\alpha + ^{24}\text{Mg}$ channel.

When the beam energy exceeds the Coulomb barrier in the $d(^{27}\text{Al}, \alpha)^{24}\text{Mg}$ entrance channel and compensates for the deuteron binding energy, the two-body $^{27}\text{Al}(p, \alpha)^{24}\text{Mg}$ reaction proceeds at astrophysically relevant energies. Given that narrow resonances dominate the

low-energy cross section, the narrow-resonance THM formalism was implemented [20, 21]. Resonance strengths are extracted in arbitrary units through peak area analysis and subsequently normalized to directly measured high-energy strengths, compensating systematic uncertainties while maintaining high accuracy. The experiment utilized an 80-MeV ^{27}Al beam on CD_2 targets with four double-sided silicon strip detectors (A–B–C–D, with A–B symmetric to D–C with respect to the beam axis) positioned to detect reaction products in coincidence. The use of two symmetric detector pairs (A–C and B–D) made it possible to cross test the experimental results and double the statistics. The experiment was carried out at the INFN Laboratori Nazionali del Sud in Catania (Italy). While all details are given in the works [22, 23], here we provide a summary of the main results.

1.4 The resonance strengths and the reaction rate

The sum of the A–C and B–D cross sections was used to derive the $d(^{27}\text{Al}, \alpha)^{24}\text{Mg}$ reaction cross section. Since the resonance widths reported in the literature are much narrower than the experimental resolution, the spectrum was fitted with a sum of Gaussian functions thus deriving the THM resonance strengths N_i [25] as the only free parameters. In the fit, resonance energies were taken from [5], and all Gaussian widths were fixed at 95 keV, as determined by Monte Carlo simulations. In the low-energy region, the dominant feature in the $d(^{27}\text{Al}, \alpha)^{24}\text{Mg}$ cross section is a resonance centered at 84.3 keV, which plays a key role in the stellar temperature range of interest. Additional resonances at 193.5 and 214.7 keV could affect the reaction rate at 0.55×10^8 K, but their fitted strengths are consistent with zero. To establish an upper limit for their contribution, the 84.3 keV peak was shifted within the energy uncertainty, and a Gaussian within the experimental uncertainties was added, yielding a combined upper limit equal to 8.6% of the 84.3 keV strength.

Because the THM strengths are determined in arbitrary units, normalization to known resonances is required. Resonances above the electron-screening region and with small uncertainties are ideal for this purpose. The peaks at 903.54 keV and 1388.8 keV were selected as reference points. Their use minimizes systematic uncertainties and model dependence, especially when employing double ratios [25]. The normalized strengths, together with their weighted averages, are listed in Tab. 1. For the unresolved resonances near 200 keV, the tabulated upper limits assume that the total THM strength is attributed to a single state, which overestimates the true limit. Dividing the strength equally between them would underestimate the constraint, as the penetration factor $P_l(kr)$ strongly depends on the orbital angular momentum.

A comparison with the literature values suggests possible revisions to the spin-parity assignments of the 705.08 keV and 855.85 keV resonances. Although previous evaluations tentatively assign $J^\pi = 2^+$ to both, the sensitivity of the strength determination to the orbital angular momentum supports a 1^- assignment for the 705.08 keV state, consistent with transfer data. The 855.85 keV state

Table 1. Strengths of the levels in the reaction $^{27}\text{Al}(p, \alpha)^{24}\text{Mg}$ in the literature and obtained in the present experiment. In column 2 the resonance energies are listed [5], in column 3 the spin-parities from [24]. Columns 4 and 5 contain the strengths and the corresponding errors, respectively, from [5], while in columns 6 and 7 the strengths and errors from [22] are given. Italic is used to highlight the presence of upper limits on the strengths.

Resonance number	E_R (keV)	J^π	$\omega\gamma^{\text{Lit.}}$ (eV)	$\delta\omega\gamma^{\text{Lit.}}$ (eV)	$\omega\gamma^{\text{THM}}$ (eV)	$\delta\omega\gamma^{\text{THM}}$ (eV)
(1)	71.5	2 ⁺	2.47×10^{-14}	-	8.23×10^{-15}	-
(2)	84.3	1 ⁻	2.60×10^{-13}	-	1.67×10^{-14}	3.2×10^{-15}
(3)	193.5	2 ⁺	3.74×10^{-7}	-	2.50×10^{-7}	-
(4)	214.7	3 ⁻	1.13×10^{-7}	-	4.36×10^{-8}	-
(5)	486.74	2 ⁺	0.11	0.05	0.107	0.021
(6)	609.49	3 ⁻	0.275	0.069	0.245	0.054
(7)	705.08	2 ⁺	0.52	0.13	0.261	0.065
(8)	855.85	2 ⁺	0.83	0.21	0.61	0.35
(9)	903.54	3 ⁻	4.3	0.4	4.20	0.38
(10)	1140.88	2 ⁺	79	27	73	14
(11)	1316.7	2 ⁺	137	47	124	28
(12)	1388.8	1 ⁻	54	15	61	12

may correspond to an unresolved 3⁻ level. The total uncertainty includes statistical errors (3–10%), integration uncertainties, peak separation errors (up to 80% for 855.85 keV), and normalization uncertainties, the latter generally being the dominant source. Resonances with large uncertainties were excluded from normalization due to their limited impact on the weighted mean.

We can conclude that the most significant outcome of this analysis is the observation and precise determination of the 84.3 keV resonance strength in the $^{27}\text{Al}(p, \alpha)^{24}\text{Mg}$ reaction, located at astrophysically relevant energies. This resonance substantially influences the reaction rate, as will be discussed in the following. Moreover, the THM-derived strengths are free from electron-screening effects, making them particularly valuable for astrophysical modeling.

For astrophysical applications, the reaction rate was computed using the Monte Carlo code RatesMC [17], which treats uncertainties statistically and incorporates Porter–Thomas and lognormal distributions. Resonance strengths were taken from Tab. 1. Unresolved states near 200 keV were treated conservatively, neglecting the 214.7 keV resonance in the recommended rate. Compared with STARLIB, our results show a reduction of about a factor of three below $T \sim 10^8$ K, mainly due to the measured 84.3 keV resonance. This substantial decrease may significantly impact the Mg–Al nucleosynthesis and the production of ^{26}Al in stellar environments as we will discuss in a later section.

2 The $^{27}\text{Al}(p, \gamma)^{28}\text{Si}$ measurement

2.1 State of the art

The $^{27}\text{Al}(p, \gamma)^{28}\text{Si}$ reaction is the obvious counterpart of the $^{27}\text{Al}(p, \alpha)^{24}\text{Mg}$, leading to the breakout from the Mg–Al cycle. Therefore, in the case of the dominance of the latter, the cycle itself would not be closed. The results in the previous section emphasized the need to further investigate the γ -channel, being necessary to quantify the interplay between the two channels. In particular,

it strongly influences elemental yields from intermediate-mass stars, particularly ^{27}Al . This is crucial for understanding the formation of multiple stellar populations in globular clusters, where AGB winds may enrich the interstellar medium from which new stars form. Building on the experimental data from [22, 23], we could provide a revised $^{27}\text{Al}(p, \gamma)^{28}\text{Si}$ reaction rate and explore its astrophysical implications. Notably, this is the first determination of the reaction rate derived directly from experimental data obtained at energies relevant to stellar nucleosynthesis.

The widely adopted $^{27}\text{Al}(p, \gamma)^{28}\text{Si}$ reaction rate [5, 10, 15] carries uncertainties of about 20% above $\sim 10^8$ K and up to an order of magnitude below it, with direct capture becoming relevant only below $\sim 0.15 \times 10^8$ K. At astrophysical energies, key contributions arise from resonances near 71.5 and 84.3 keV, for which only upper limits are available from reanalyzed stripping data [26]. Slightly higher in energy, an unresolved triplet near 193–195 keV contributes. Improved spectroscopic information on these threshold states has previously altered the reaction rate by up to a factor of 20 below 0.7×10^8 K, highlighting their astrophysical significance.

2.2 The THM resonance strengths at low energies

The THM results about the $^{27}\text{Al}(p, \alpha)^{24}\text{Mg}$ reaction [22, 23] enabled the precise determination of the 84.3 keV resonance strength and a new, ~ 3 times lower upper limit for the 71.5 keV resonance. These results allow the derivation of new experimental estimates of the $^{27}\text{Al}(p, \gamma)^{28}\text{Si}$ resonance strengths, particularly for the low-energy resonances crucial to astrophysical modeling. Here we discuss the resonance strengths or the revised upper limits up to about 200 keV, while a more exhaustive discussion is presented in [27]. Our considerations are based on the definition of resonance strengths [4], given the fact that direct capture is relevant only at very low temperatures (see above).

For the 71.5 keV resonance, the hierarchy $\Gamma_p \ll \Gamma_\gamma \ll \Gamma_\alpha$ implies that the (p, α) strength is proportional to Γ_p . A

more stringent THM limit on this width leads to a corresponding upper limit on the (p, γ) strength of 2×10^{-15} eV. The 84.3 keV resonance behaves differently, with $\Gamma_p \ll \Gamma_\gamma \sim \Gamma_\alpha$, making both (p, α) and (p, γ) strengths proportional to Γ_p . From THM data, $\Gamma_p = (1.67 \pm 0.59) \times 10^{-13}$ eV, yielding a (p, γ) strength of $(2.5 \pm 1.3) \times 10^{-14}$ eV. For this resonance, only upper limits were available in the literature, as in the case of the (p, α) channel. The unresolved triplet near 193–195.5 keV complicates strength determination. Literature values are retained here due to ambiguities in channel assignment. Finally, for the 214.7 keV resonance, where $\Gamma_p \ll \Gamma_\alpha \ll \Gamma_\gamma$, the main uncertainty lies in Γ_α . Since THM data provide only an upper limit, the literature strength is adopted. Overall, THM measurements significantly refine the low-energy resonance strengths, particularly the 84.3 keV state, improving the constraints on the $^{27}\text{Al}(p, \gamma)^{28}\text{Si}$ reaction rate relevant to stellar nucleosynthesis.

To summarize the results, in Fig. 2 we show the ratios between the $^{27}\text{Al}(p, \alpha)^{24}\text{Mg}$ and the $^{27}\text{Al}(p, \gamma)^{28}\text{Si}$ reaction rates calculated from the application of the THM [22, 27] (red band) and taken from Ref. [10] (green band). In the figure, errors are from the $((p, \alpha)$ channel only (comparable errors affect the $((p, \gamma)$ channel). Fig. 2 shows that, while the THM rates are both lower than what given in the literature, the ratios are in good agreement with each other.

3 Astrophysical implications of the updated $^{27}\text{Al}+p$ reaction network

The branching between the $^{27}\text{Al}(p, \alpha)^{24}\text{Mg}$ and $^{27}\text{Al}(p, \gamma)^{28}\text{Si}$ channels regulates the leakage from the Mg–Al cycle toward silicon and determines whether aluminium is efficiently depleted or instead accumulated during hydrogen-burning episodes in stellar interiors (see Fig. 1). Our assessment of the $^{27}\text{Al}(p, \alpha)^{24}\text{Mg}$ rate illustrates that the revised 84.3 keV resonance strengths reduces the temperature interval in which the (p, α) channel dominates to $(0.17 \leq T_9 \leq 0.27) \times 10^8$ K, whereas

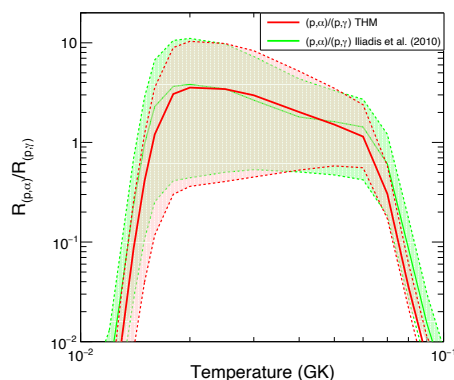


Figure 2. Comparison of the ratios between the $^{27}\text{Al}(p, \alpha)^{24}\text{Mg}$ and the $^{27}\text{Al}(p, \gamma)^{28}\text{Si}$ reaction rates calculated from the application of the THM [22, 27] (red band) and taken from Ref. [10] (green band). Dotted lines and dashed areas are used to highlight the uncertainties, that are given for the $((p, \alpha)$ channel only.

the previously adopted rates from [5] allowed for a wider contribution of this channel. Such a revision implies a reduced efficiency of the $^{27}\text{Al}(p, \alpha)^{24}\text{Mg}$ depletion at low temperatures, which in turn affects stellar models where hydrogen burning proceeds under marginal thermal conditions.

It is also important to underscore that lower (p, γ) and (p, α) channels reaction rates may cause a lower ^{27}Al destruction rate and an enhanced surface aluminium abundance. On the other hand, a minor impact on the ^{24}Mg and ^{28}Si reservoir may be expected as both isotopes are not dominantly produced in H-burning processes.

To assess these implications, we focused on asymptotic giant branch (AGB) stars in the initial mass range 4–8 M_\odot , which undergo hot bottom burning (HBB) during their thermally pulsing phase. In these stars, the convective envelope penetrates deeply into regions hot enough to activate proton-capture nucleosynthesis, with the temperature at the base of the convective envelope (T_{bce}) being the key parameter controlling the activation of the Mg–Al cycle. We computed full evolutionary models at solar metallicity ($Z = 0.014$) using the ATON stellar evolution code [28], adopting a 4.5 M_\odot model as representative of mild HBB conditions and a 6 M_\odot model as a case where HBB operates efficiently with T_{bce} exceeding $\sim 0.8 \times 10^8$ K.

For the 6 M_\odot model, the high temperatures achieved ensure that the (p, γ) channel overwhelmingly contributes to the depletion of ^{27}Al , driving the reaction flow toward ^{28}Si . In this regime, differences between the reaction rates adopted here and those from the STARLIB database are negligible, resulting in virtually identical surface abundances. However, the situation differs significantly in the 4.5 M_\odot model, for which T_{bce} remains around $\sim 0.7 \times 10^8$ K. Under these conditions, the (p, α) channel plays a non-negligible role, and the reduced efficiency imposed by the updated rate leads to a slight but measurable enhancement of surface aluminium. Specifically, we find an increase of approximately 5% in the surface abundance of ^{27}Al when adopting the recommended reaction rate. When the lower limit of the rate is considered, this increment can reach up to $\sim 25\%$, reflecting the sensitivity of the nucleosynthetic outcome to the assumed resonance strengths.

The impact on ^{24}Mg is more modest, as its initial abundance largely exceeds that of ^{27}Al . Consequently, even small variations in the destruction rate of ^{27}Al do not significantly alter the ^{24}Mg reservoir. This results in minor changes to the $^{24}\text{Mg}/^{27}\text{Al}$ ratio, which remains within the uncertainties typically adopted in chemical evolution models of AGB ejecta. Nonetheless, even moderate enhancements in aluminium production may have observational relevance. In fact, AGB stars have been proposed as polluters responsible for the chemical anomalies observed in multiple populations of globular clusters, especially regarding light elements such as Mg, Al, and Si. The revised reaction rate supports scenarios in which intermediate-mass AGB stars contribute to the observed aluminium enrichment without producing excessive silicon, as would occur if the (p, γ) channel were too dominant.

In summary, the updated $^{27}\text{Al}(p,\alpha)^{24}\text{Mg}$ and $^{27}\text{Al}(p,\gamma)^{28}\text{Si}$ reaction rates derived from THM-based resonance strengths mildly favors aluminium production in AGB stars experiencing marginal HBB. This result refines the nucleosynthesis yields used in globular cluster enrichment models and highlights the relevance of accurate low-energy resonance strength determinations for stellar nucleosynthesis studies. More work is ongoing to better establish the astrophysical impact in low-mass AGB stars.

References

- [1] K. Lind, S.E. Koposov, C. Battistini, A.F. Marino, G. Ruchti, A. Serenelli, C.C. Worley, A. Alves-Brito, M. Asplund, P.S. Barklem et al., The Gaia-ESO Survey: A globular cluster escapee in the Galactic halo, *Astron. Astrophys.* **575**, L12 (2015), 1502.03934. [10.1051/0004-6361/201425554](https://doi.org/10.1051/0004-6361/201425554)
- [2] G.S. Da Costa, J.E. Norris, D. Yong, Magnesium Isotope Ratios in ω Centauri Red Giants, *Astrophysical Journal* **769**, 8 (2013), 1304.0523. [10.1088/0004-637X/769/1/8](https://doi.org/10.1088/0004-637X/769/1/8)
- [3] D. Yong, F. Grundahl, D.L. Lambert, P.E. Nissen, M.D. Shetrone, Mg isotopic ratios in giant stars of the globular cluster NGC 6752, *Astron. Astrophys.* **402**, 985 (2003), astro-ph/0303057. [10.1051/0004-6361:20030296](https://doi.org/10.1051/0004-6361:20030296)
- [4] C. Iliadis, Nuclear physics of stars (Weinheim, Wiley-VCH Verlag GmbH & Co, 2015)
- [5] C. Iliadis, R. Longland, A.E. Champagne, A. Coc, Charged-particle thermonuclear reaction rates: III. Nuclear physics input, *Nucl. Phys.* **A841**, 251 (2010), 1004.4149. [10.1016/j.nuclphysa.2010.04.010](https://doi.org/10.1016/j.nuclphysa.2010.04.010)
- [6] R. Diehl, H. Halloin, K. Kretschmer, G.G. Lichti, V. Schönfelder, A.W. Strong, A. von Kienlin, W. Wang, P. Jean, J. Knödseder et al., Radioactive ^{26}Al from massive stars in the Galaxy, *Nature* **439**, 45 (2006), astro-ph/0601015. [10.1038/nature04364](https://doi.org/10.1038/nature04364)
- [7] E. Groopman, E. Zinner, S. Amari, F. Gyngard, P. Hoppe, M. Jadhav, Y. Lin, Y. Xu, K. Marhas, L.R. Nittler, Inferred Initial $^{26}\text{Al}/^{27}\text{Al}$ Ratios in Presolar Stardust Grains from Supernovae are Higher than Previously Estimated, *Astrophysical Journal* **809**, 31 (2015). [10.1088/0004-637X/809/1/31](https://doi.org/10.1088/0004-637X/809/1/31)
- [8] C. Iliadis, A. Champagne, A. Chieffi, M. Limongi, The Effects of Thermonuclear Reaction Rate Variations on ^{26}Al Production in Massive Stars: A Sensitivity Study, *Astrophysical Journal Supplement Series* **193**, 16 (2011), 1101.5553. [10.1088/0067-0049/193/1/16](https://doi.org/10.1088/0067-0049/193/1/16)
- [9] S. Palmerini, O. Trippella, M. Busso, A deep mixing solution to the aluminum and oxygen isotope puzzles in pre-solar grains, *Monthly Notices of the RAS* **467**, 1193 (2017), 1701.04445. [10.1093/mnras/stx137](https://doi.org/10.1093/mnras/stx137)
- [10] C. Iliadis, R. Longland, A.E. Champagne, A. Coc, R. Fitzgerald, Charged-particle thermonuclear reaction rates: II. Tables and graphs of reaction rates and probability density functions, *Nucl. Phys.* **A841**, 31 (2010), 1004.4517. [10.1016/j.nuclphysa.2010.04.009](https://doi.org/10.1016/j.nuclphysa.2010.04.009)
- [11] R. Timmermann, H.W. Becker, C. Rolfs, U. Schröder, H.P. Trautvetter, Search for low-energy resonances in $^{27}\text{Al}(p, \alpha)^{24}\text{Mg}$, *Nucl. Phys.* **A477**, 105 (1988). [10.1016/0375-9474\(88\)90363-6](https://doi.org/10.1016/0375-9474(88)90363-6)
- [12] P.M. Endt, Supplement to energy levels of A = 21-44 nuclei (VII), *Nucl. Phys.* **A633**, 1 (1998). [10.1016/S0375-9474\(97\)00613-1](https://doi.org/10.1016/S0375-9474(97)00613-1)
- [13] A.E. Champagne, C.H. Cella, R.T. Kouzes, M.M. Lowry, P.V. Magnus, M.S. Smith, Z.Q. Mao, Particle decays in ^{28}Si : The destruction of ^{27}Al in red giants and novae, *Nucl. Phys.* **A487**, 433 (1988). [10.1016/0375-9474\(88\)90622-7](https://doi.org/10.1016/0375-9474(88)90622-7)
- [14] P.M. Endt, J.G.L. Booten, The shell model for T = 0 and T = 1 states in the middle of the sd shell, *Nucl. Phys.* **A555**, 499 (1993). [10.1016/0375-9474\(93\)90486-H](https://doi.org/10.1016/0375-9474(93)90486-H)
- [15] C. Iliadis, J.M. D'Auria, S. Starrfield, W.J. Thompson, M. Wiescher, Proton-induced Thermonuclear Reaction Rates for A=20-40 Nuclei, *Astrophysical Journal Supplement Series* **134**, 151 (2001). [10.1086/320364](https://doi.org/10.1086/320364)
- [16] C. Angulo, M. Arnould, M. Rayet, P. Descouvement, D. Baye, C. Leclercq-Willain, A. Coc, S. Barhoumi, P. Aguer, C. Rolfs et al., A compilation of charged-particle induced thermonuclear reaction rates, *Nucl. Phys.* **A656**, 3 (1999). [10.1016/S0375-9474\(99\)00030-5](https://doi.org/10.1016/S0375-9474(99)00030-5)
- [17] R. Longland, C. Iliadis, A.E. Champagne, J.R. Newton, C. Ugalde, A. Coc, R. Fitzgerald, Charged-particle thermonuclear reaction rates: I. Monte Carlo method and statistical distributions, *Nucl. Phys.* **A841**, 1 (2010), 1004.4136. [10.1016/j.nuclphysa.2010.04.008](https://doi.org/10.1016/j.nuclphysa.2010.04.008)
- [18] S. Cristallo, M. La Cognata, C. Massimi, A. Best, S. Palmerini, O. Straniero, O. Trippella, M. Busso, G.F. Ciani, F. Mingrone et al., The Importance of the $^{13}\text{C}(\alpha,n)^{16}\text{O}$ Reaction in Asymptotic Giant Branch Stars, *Astrophysical Journal* **859**, 105 (2018), 1804.10751. [10.3847/1538-4357/aac177](https://doi.org/10.3847/1538-4357/aac177)
- [19] A. Tumino, C.A. Bertulani, M. La Cognata, L. Lamia, R.G. Pizzone, S. Romano, S. Typel, The Trojan Horse Method: A Nuclear Physics Tool for Astrophysics, *Annual Review of Nuclear and Particle Science* **71**, 345 (2021). [10.1146/annurev-nucl-102419-033642](https://doi.org/10.1146/annurev-nucl-102419-033642)
- [20] M. La Cognata, C. Spitaleri, A.M. Mukhamedzhanov, B. Irgaziev, R.E. Tribble, A. Banu, S. Cherubini, A. Coc, V. Crucillà, V.Z. Goldberg et al., Measurement of the 20 and 90keV Resonances in the $\text{O}18(p,\alpha)\text{N}15$ Reaction via the Trojan Horse Method, *Phys. Rev. Lett.* **101**, 152501 (2008), 0806.1274. [10.1103/PhysRevLett.101.152501](https://doi.org/10.1103/PhysRevLett.101.152501)
- [21] M.L. Sergi, C. Spitaleri, M. La Cognata, L. Lamia, R.G. Pizzone, G.G. Rapisarda, X.D. Tang, B. Bucher, M. Couder, P. Davies et al., Improvement

- of the high-accuracy $^{17}\text{O}(p, \alpha)^{14}\text{N}$ reaction-rate measurement via the Trojan Horse method for application to ^{17}O nucleosynthesis, *Phys. Rev. C* **91**, 065803 (2015). [10.1103/PhysRevC.91.065803](https://doi.org/10.1103/PhysRevC.91.065803)
- [22] M. La Cognata, S. Palmerini, P. Adsley, F. Hammache, A. Di Pietro, P. Figuera, F. Dell’Agli, R. Alba, S. Cherubini, G.L. Guardo et al., A New Reaction Rate of the $^{27}\text{Al}(p,\alpha)^{24}\text{Mg}$ Reaction Based on Indirect Measurements at Astrophysical Energies and Implications for ^{27}Al Yields of Intermediate-mass Stars, *Astrophysical Journal* **941**, 96 (2022). [10.3847/1538-4357/ac9c5e](https://doi.org/10.3847/1538-4357/ac9c5e)
- [23] M. La Cognata, S. Palmerini, P. Adsley, F. Hammache, A. Di Pietro, P. Figuera, R. Alba, S. Cherubini, F. Dell’Agli, G.L. Guardo et al., Exploring the astrophysical energy range of the $^{27}\text{Al}(p,\alpha)^{24}\text{Mg}$ reaction: A new recommended reaction rate, *Physics Letters B* **826**, 136917 (2022). [10.1016/j.physletb.2022.136917](https://doi.org/10.1016/j.physletb.2022.136917)
- [24] A.A. Sonzogni, NuDat 2.0: Nuclear Structure and Decay Data on the Internet, in *International Conference on Nuclear Data for Science and Technology*, edited by R.C. Haight, M.B. Chadwick, T. Kawano, P. Talou (AIP, 2005), Vol. 769 of *American Institute of Physics Conference Series*, pp. 574–577
- [25] M. La Cognata, C. Spitaleri, A. Mukhamedzhanov, A. Banu, S. Cherubini, A. Coc, V. Crucillà, V. Goldberg, M. Gulino, B. Irgaziev et al., A Novel Approach to Measure the Cross Section of the $^{18}\text{O}(p, \alpha)^{15}\text{N}$ Resonant Reaction in the 0-200 keV Energy Range, *Astrophysical Journal* **708**, 796 (2010). [10.1088/0004-637X/708/1/796](https://doi.org/10.1088/0004-637X/708/1/796)
- [26] A.E. Champagne, M.L. Pitt, P.H. Zhang, L.L. Lee, M.J. Levine, Proton-threshold states in ^{28}Si , *Nucl. Phys. A* **459**, 239 (1986). [10.1016/0375-9474\(86\)90065-5](https://doi.org/10.1016/0375-9474(86)90065-5)
- [27] M. La Cognata, S. Palmerini, F. Dell’Agli, P. Ventura, P. Adsley, R. Alba, S. Cherubini, M. Costa, A. Di Pietro, P. Figuera et al., A New Reaction Rate of the $^{27}\text{Al}(p,\gamma)^{28}\text{Si}$ Reaction Based on Indirect Low-energy Cross-section Measurements, *Astrophysical Journal* **982**, 91 (2025). [10.3847/1538-4357/adb7e4](https://doi.org/10.3847/1538-4357/adb7e4)
- [28] P. Ventura, F. D’Antona, I. Mazzitelli, The ATON 3.1 stellar evolutionary code. A version for asteroseismology, *Astrophysics and Space Science* **316**, 93 (2008). [10.1007/s10509-007-9672-8](https://doi.org/10.1007/s10509-007-9672-8)